Development 136, 2825-2835 (2009) doi:10.1242/dev.038505

Conditional inactivation of *Has2* reveals a crucial role for hyaluronan in skeletal growth, patterning, chondrocyte maturation and joint formation in the developing limb

Kazu Matsumoto[1,*], Yingcui Li[2,*], Caroline Jakuba[2], Yoshinori Sugiyama[1,3], Tetsuya Sayo[3], Misako Okuno[1], Caroline N. Dealy[2], Bryan P. Toole[4], Junji Takeda[5], Yu Yamaguchi[1,†] and Robert A. Kosher[2,†]

The glycosaminoglycan hyaluronan (HA) is a structural component of extracellular matrices and also interacts with cell surface receptors to directly influence cell behavior. To explore functions of HA in limb skeletal development, we conditionally inactivated the gene for HA synthase 2, *Has2*, in limb bud mesoderm using mice that harbor a floxed allele of *Has2* and mice carrying a limb mesoderm-specific *Prx1-Cre* transgene. The skeletal elements of *Has2*-deficient limbs are severely shortened, indicating that HA is essential for normal longitudinal growth of all limb skeletal elements. Proximal phalanges are duplicated in *Has2* mutant limbs indicating an involvement of HA in patterning specific portions of the digits. The growth plates of *Has2*-deficient skeletal elements are severely abnormal and disorganized, with a decrease in the deposition of aggrecan in the matrix and a disruption in normal columnar cellular relationships. Furthermore, there is a striking reduction in the number of hypertrophic chondrocytes and in the expression domains of markers of hypertrophic differentiation in the mutant growth plates, indicating that HA is necessary for the normal progression of chondrocyte maturation. In addition, secondary ossification centers do not form in the central regions of *Has2* mutant growth plates owing to a failure of hypertrophic differentiation. In addition to skeletal defects, the formation of synovial joint cavities is defective in *Has2*-deficient limbs. Taken together, our results demonstrate that HA has a crucial role in skeletal growth, patterning, chondrocyte maturation and synovial joint formation in the developing limb.

KEY WORDS: Hyaluronan, Has2, Chondrocyte maturation, Joint development, Skeletal development, Limb development, Mouse

INTRODUCTION

Hyaluronan (HA) is a linear glycosaminoglycan composed of repeating disaccharide units of D-glucuronic acid and N-acetyl-D-glucosamine. It is a huge molecule, with a molecular weight ranging from 10^3 to 10^4 kDa and an extended length of 2-25 μm (Toole, 1997; Toole, 2000a; Toole, 2000b). HA is a structural component of the extracellular matrix of a variety of tissues. However, HA is not simply a passive structural and space-filling component of extracellular matrices. Rather, HA directly interacts with cells to influence their behavior. HA has been implicated in the regulation of multiple biological processes including wound healing, angiogenesis, branching morphogenesis, tumor metastasis, cell migration and proliferation (Gakunga et al., 1997; Weigel et al., 1997; Toole et al., 2001).

HA occupies a very large molecular domain in dilute solution and has a pronounced hydration capacity (Toole, 1997; Toole, 2000a; Toole, 2000b). At higher concentrations, individual extended HA molecules form an entangled continuous hydrated network that is thought to facilitate cell migration and proliferation (Toole, 1997; Toole, 2000a; Toole, 2000b). Although several of the functions of HA may be attributable to these physicochemical properties, HA also interacts with specific cell surface receptors or binding proteins called hyaladherins to directly regulate cellular processes. The major cell surface receptor for HA is CD44, which is an integral membrane protein containing an extracellular domain, the N-terminus of which binds HA, and a short cytoplasmic domain associated with the cytoskeleton (Toole, 1997; Toole, 2000b). HA can also bind to several other hyaladherins, most notably Rhamm (Hmmr – Mouse Genome Informatics), which has been implicated in cell motility (Tammi et al., 2002). Interaction of HA with its major cell surface receptor CD44 often results in the formation of stable HA-rich pericellular coats that influence cell behavior (Toole, 1997; Toole, 2000b).

Interaction of HA with its cell surface receptors, including CD44, can directly activate intracellular signaling pathways that regulate various cellular activities (Turley et al., 2000). HA is an important modulator or co-activator of the EGFR/ErbB (Bourguignon et al., 1997; Sherman et al., 2000; Camenisch et al., 2002; Tsatas et al., 2002; Ghatak et al., 2005; Misra et al., 2005), TGFβ (Bourguignon et al., 2002) and BMP (Peterson et al., 2004) signaling networks, and acts in concert with these signaling molecules to regulate a variety of cellular processes. In addition, HA constitutively regulates the activation of other receptor tyrosine kinases including IGF1Rβ, PDGFRβ and c-MET in human colon, prostate and breast carcinoma cells (Misra et al., 2006).

HA is synthesized in a unique fashion. It is produced at the inner side of the plasma membrane rather than in the Golgi apparatus and is extruded to the outside of the cell during polymerization (Weigel et al., 1997). HA is synthesized by three HA synthase isoforms: Has1, Has2 and Has3 (Weigel et al., 1997; Spicer and McDonald, 1998). Each of the Has enzymes exhibits both of the glycosyltransferase activities required for HA synthesis. The three

[1]Sanford Children's Health Research Center, Burnham Institute for Medical Research, La Jolla, CA 92037, USA. [2]Center for Regenerative Medicine and Skeletal Development, Department of Orthopaedic Surgery and University of Connecticut Stem Cell Institute, University of Connecticut Health Center, Farmington, CT 06030, USA. [3]Basic Research Laboratory, Kanebo Cosmetics, Odawara 250-0002, Japan. [4]Department of Cell Biology and Anatomy, Medical University of South Carolina, Charleston, SC 29425, USA. [5]Department of Social and Environmental Medicine, Graduate School of Medicine, Osaka University, Osaka 565-0871, Japan.

*These authors contributed equally to this work
†Authors for correspondence (e-mails: yyamaguchi@burnham.org; rakosher@snet.net)

Accepted 9 June 2009

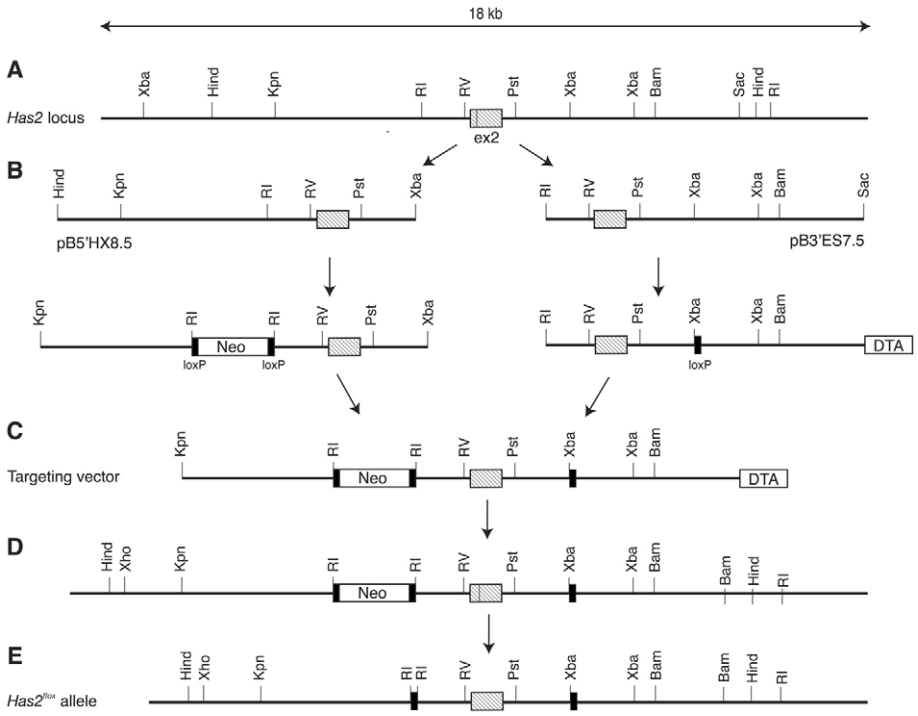

Fig. 1. Creation of the *Has2*^{flox} allele. (**A**) Map of the mouse *Has2* locus surrounding exon 2. (**B**) Two genomic fragments (pB5′HX8.5 and pB3′ES7.5) spanning exon 2 were isolated from a BAC library and modified by introducing selection markers and loxP sequences. (**C**) The structure of the targeting vector assembled from pB5′HX8.5 and pB3′ES7.5. (**D**) The *Has2* locus after homologous recombination. (**E**) The *Has2*^{flox} locus after in vivo elimination of the Neo cassette. ex2, exon 2; Neo, neomycin; DTA, diphtheria toxin A.

HA synthases exhibit distinct expression patterns during mouse development (Spicer and McDonald, 1998) and have distinctly different enzymatic properties (Itano et al., 1999). There might be functional differences between the HA synthesized by the different synthases (Spicer and McDonald, 1998; Itano et al., 1999). Has2 is the major source of HA during early organogenesis in the mouse embryo, HA being virtually absent from the embryos of *Has2*-null mice, which die at mid-gestation (E9.5-10) (Camenisch et al., 2000). By contrast, mice lacking one or both of the *Has1* and *Has3* genes are viable and exhibit no obvious phenotype. Thus, Has2 is the crucial synthase for HA biosynthesis in development.

HA has been implicated in various aspects of limb morphogenesis. The distal subridge mesenchymal cells of the developing limb bud that undergo proliferation, directed migration and patterning in response to the apical ectodermal ridge (AER) abundantly express *Has2* (Li et al., 2007) and produce high amounts of HA, which forms an expansive hydrated extracellular matrix between the cells (Kosher et al., 1981; Singley and Solursh, 1981). *Has2* is also abundantly expressed by the AER itself (Li et al., 2007), and large amounts of HA are secreted by the AER (Kosher and Savage, 1981). Thus, the cell and tissue interactions that control the outgrowth and patterning of the limb occur in an environment that is rich in extracellular and pericellular HA, which has the potential to be involved in regulating these processes. *Has2* expression and HA production are downregulated in the proximal central core of the limb bud during the formation of the precartilage condensations of the limb skeletal elements in which the cell-cell interactions occur that trigger cartilage differentiation (Kosher et al., 1981; Knudson and Toole, 1985). Overexpression of *Has2* in the mesoderm of the chick limb bud in vivo results in the formation of shortened and severely malformed limbs that lack one or more skeletal elements and/or possess skeletal elements that exhibit abnormal morphology and are positioned inappropriately (Li et al., 2007). Thus, sustained production of HA in vivo perturbs limb growth, patterning and cartilage differentiation. Furthermore, sustained HA production in micromass cultures of limb mesenchymal cells inhibits the formation of precartilage condensations and subsequent chondrogenesis, indicating that downregulation of HA is necessary for the formation of the precartilage condensations that trigger cartilage differentiation (Li et al., 2007).

The mid-gestation lethality of conventional *Has2*-null embryos has hindered a thorough evaluation of the functions of HA in limb and skeletal development. Accordingly, in the present study we have performed tissue-specific inactivation of the *Has2* gene in mouse limb bud mesoderm using mice that harbor a floxed allele of *Has2* and mice carrying a limb mesoderm-specific *Prx1-Cre* transgene (Logan et al., 2002). Our analysis of the phenotype of the *Has2*-deficient limbs indicates that Has2-mediated production of HA plays a crucial role in skeletal growth, patterning, chondrocyte maturation and synovial joint formation.

MATERIALS AND METHODS

Generation of conditional *Has2* knockout mice

Two mouse genomic clones containing exon 2 of the *Has2* gene, namely pB5′HX8.5 extending toward the 5′ end and pB3′ES7.5 extending toward the 3′ end, were isolated from a BAC library derived from 129SvJ mice (Fig. 1). Exon 2 contains the start codon and two transmembrane domains located in the N-terminal region. pB5′HX8.5 was introduced with a neomycin (Neo) selection cassette flanked by two loxP sites, and pB3′ES7.5 was modified with a loxP site and a diphtheria toxin A (DTA) selection cassette. These two fragments were assembled into a targeting vector (Fig. 1B), which was electroporated into the R1 mouse embryonic stem cell line. After G418/DTA double selection, clones that had undergone homologous recombination were identified by PCR and Southern blotting. Chimeric mice were generated from one of the homologous recombinant clones by aggregation (Woods et al., 1993) and backcrossed with C57BL/6 mice to generate heterozygous mice carrying the targeted *Has2* allele. The Neo selection cassette was then removed in vivo by crossing the heterozygous mice with *EIIa-Cre* transgenic mice (Lasko et al., 1996). The resultant *Has2* allele is designated *Has2*^{flox} in this paper. Homozygous mice carrying the *Has2*^{flox} alleles develop and reproduce without any obvious phenotype, confirming that the *Has2*^{flox} allele is functional.

To produce *Has2* conditional knockout mice targeted to the mesoderm of developing limb buds, the *Prx1-Cre* transgene, which drives recombination in early limb bud mesenchyme (Logan et al., 2002), was introduced into $Has2^{flox/+}$ mice. Resultant $Prx1\text{-}Cre;Has2^{flox/wt}$ male mice were mated with $Has2^{flox/flox}$ female mice to obtain *Has2* conditional knockout mice ($Prx1\text{-}Cre;Has2^{flox/flox}$). Littermates that inherited the incomplete combination of the above alleles were used as controls (referred to as wild type). Genotyping of the mice and embryos was by PCR using DNA prepared from tail biopsies and yolk sacs. All protocols for animal use were approved by the IACUC of the Burnham Institute for Medical Research and the University of Connecticut Health Center, and were in accordance with NIH guidelines.

In situ hybridization

In situ hybridization on serially sectioned tissue that had been fixed in 4% paraformaldehyde was performed with ^{33}P- or digoxigenin-labeled probes as previously described (Coelho et al., 1991; Inatani et al., 2003; Matsumoto et al., 2007). The probes included mouse *Ihh* (gift of C. Tabin, Harvard Medical School, Boston, MA, USA and K. Muneoka, Tulane University, New Orleans, LA, USA) and mouse *Col10a1* (gift of B. Olsen and C. Tabin, Harvard Medical School, Boston, MA, USA). A 752 bp *Has2* cDNA probe extending from nucleotides 1461 to 2212 at the 3′ end of the cDNA was prepared by digesting a pCI-Neo vector containing the complete coding sequence of mouse *Has2* (GenBank accession number NM_008216) with *Xma*I and *Eco*R1. A 207 bp mouse *Has2* exon 2-specifc probe extending from nucleotides 873 to 1079 was prepared by PCR. To precisely correlate expression with various cell populations, dark-field and bright-field images of the same ^{33}P-labeled sections were acquired, silver grains representing the expression domains were selected in the dark-field images using the Color Range command in Adobe Photoshop (version 7.0), pseudocolored red, and superimposed on the Hematoxylin-stained bright-field images of the same sections.

Staining

Whole-mount skeletal staining with Alcian Blue and Alizarin Red to visualize cartilage and mineralized bone was performed essentially as described by McLeod (McLeod, 1980). Safranin O staining of glycosaminoglycans was performed by staining sections with Weigert's Iron Hematoxylin and 0.02% aqueous Fast Green, followed by rinsing with 1% acetic acid and staining with 0.1% aqueous Safranin O.

Cell proliferation assay

Immunostaining for phosphorylated histone H3 (pHistoneH3) to assay cell proliferation was performed as previously described (Fisher et al., 2007) using a polyclonal antibody to the serine 10 phosphorylated form of histone H3 (Upstate). The numbers of pHistoneH3-labeled and -unlabeled nuclei were counted in adjacent sections through the middle of the metaphyseal regions of the proximal and distal humerus of wild-type and *Has2*-deficient E16.5 embryos.

Immunostaining

Immunostaining was performed using mouse anti-aggrecan monoclonal antibody 1C6 (Developmental Studies Hybridoma Bank, Iowa City, IA, USA), rabbit anti-type II collagen antibody (Research Diagnostics, Concord, MA, USA) and rat anti-CD31 antibody (SouthernBiotech, Birmingham, AL, USA). Prior to immunostaining for aggrecan and type II collagen, sections were pretreated with chondroitinase ABC (0.05 units/ml; Seikagaku, Tokyo, Japan) and hyaluronidase (2.5%; Sigma), respectively. Secondary antibodies used were biotinylated goat anti-mouse IgG antibody (Zymed Laboratories, South San Francisco, CA, USA), Alexa Fluor 488-conjugated goat anti-rabbit IgG antibody (Invitrogen, Carlsbad, CA, USA) and horseradish peroxidase-conjugated goat anti-rat IgG antibody (Vector Laboratories, Burlingame, CA, USA). For immunostaining of aggrecan, the HistoMouse Kit (Zymed Laboratories) was used. In the case of horseradish peroxidase-based detection, sections were quenched with 0.3% hydrogen peroxide prior to incubation with primary antibodies. After immunostaining, some sections were counterstained with Hematoxylin or DAPI.

Distribution of HA

The distribution of HA was determined as previously described (Li et al., 2007) by histochemical staining with biotinylated HA-binding protein (HABP) (Seikagaku American) from the HA-binding region of aggrecan, which binds strongly and specifically to HA in tissue sections. Prior to HABP staining, sections were pretreated with 0.05% trypsin for 30 minutes at room temperature and 0.25-1 unit/ml chondroitinase ABC (Seikagaku American) for 1 hour at 37°C. No HABP staining was detectable in alternate sections pretreated for 2 hours at 60°C with 200 TRU/ml *Streptomyces hyalurolyticus* hyaluronidase (Seikagaku American), which specifically degrades HA.

RESULTS

Conditional inactivation of *Has2* in limb bud mesoderm results in the formation of severely shortened limb skeletal elements

The *Has2* gene was conditionally inactivated in limb mesoderm using mice that we generated to harbor a floxed *Has2* allele (Fig. 1) and mice carrying a limb mesoderm-specific *Prx1-Cre* transgene (Logan et al., 2002). The *Has2* floxed mice possess a *Has2* allele with loxP sites flanking exon 2, which includes the

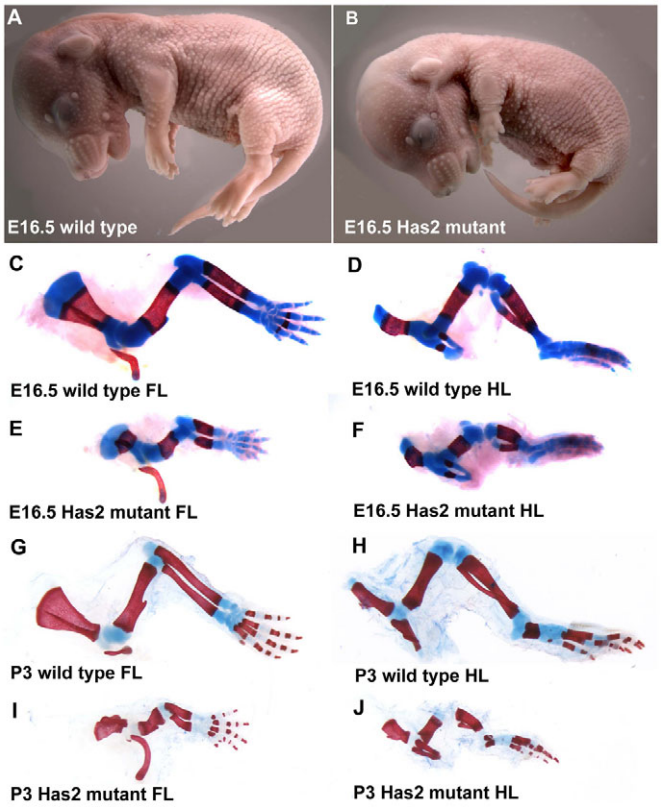

Fig. 2. Has2-mediated production of HA is essential for normal longitudinal growth of limb skeletal elements. (**A**,**B**) E16.5 wild-type mouse embryo (A) and an embryo in which *Has2* was conditionally inactivated in limb mesoderm (Has2 mutant) (B). The limbs of the *Has2* mutant are extremely shortened. (**C-J**) Alcian Blue/Alizarin Red-stained skeletal elements of E16.5 (C-F) and P3 (G-J) wild-type (C,D,G,H) and *Has2*-deficient (E,F,I,J) forelimbs (C,E,G,I) and hindlimbs (D,F,H,J). The skeletal elements in each of the segments of the *Has2*-deficient mutant limbs are severely shortened, and the *Has2*-deficient skeletal elements stain less intensely with Alcian Blue, suggesting a defect in the deposition of sulfated proteoglycans in the matrix. FL, forelimb; HL, hindlimb.

start codon and two N-terminal transmembrane domains crucial for insertion of Has2 into the plasma membrane, and the allele acts as a null allele upon Cre-mediated recombination. Cre recombinase driven by the *Prx1* (*Prrx1*) enhancer is first detectable in limb bud mesoderm at E9.5 and is expressed in all of the mesenchymal cells of the limb at E10.5, but not in limb ectoderm (Logan et al., 2002). As described in detail below, in the limbs of *Has2*-deficient mutant embryos, *Has2* transcript expression is not detectable by in situ hybridization using an exon 2-specific probe, and little HA is detectable by staining with biotinylated hyaluronic acid-binding protein (HABP).

As shown in Fig. 2, E16.5 embryos in which the *Has2* gene was conditionally inactivated in limb mesoderm possessed extremely shortened limbs compared with wild-type littermates. However, in all other respects the gross appearance of the mutant embryos and neonates appeared essentially normal (Fig. 2A,B). Alcian Blue/Alizarin Red whole-mount staining to visualize cartilage and mineralized bone, respectively, confirmed that the forelimbs and hindlimbs of the *Has2* mutant E16.5 embryos and neonates were severely shortened and malformed (Fig. 2). The skeletal elements in each of the segments (stylopod, zeugopod and autopod) of the *Has2*-deficient mutant forelimbs and hindlimbs at E16.5 and P3 were about half the length of those of normal littermates (Fig. 2). In addition to being severely shortened, the *Has2* mutant skeletal elements stained less intensely with Alcian Blue, suggesting a defect in the deposition of sulfated proteoglycans in the cartilage matrix (Fig. 2). These skeletal defects were observed with 100% penetrance in more than 30 mutant embryos and neonates examined. Despite these severe skeletal defects, *Has2* mutant mice are capable of locomotion in a manner similar to that of pinnipeds.

Skeletal patterning defects in the autopods of *Has2*-deficient limbs

In addition to being severely shortened and exhibiting decreased Alcian Blue staining, *Has2*-deficient mutant limbs exhibited specific skeletal patterning defects. As shown in the higher magnification image of the forelimb autopods of E16.5 limbs in Fig. 3, the proximal phalanges of digits 2 and 5 were duplicated and misshapen in the *Has2*-deficient autopods (see also Fig. 4B,D). The proximal phalanges of digits 2 and 5 were duplicated in both the left and right forelimbs and hindlimbs of all of the *Has2* mutants we have examined at E16.5. At P0, 100% of the *Has2* mutants exhibited duplications of the proximal phalanges of digits 2 and 5, and ~53% (8/15) also exhibited partial duplications of the proximal phalanges of digits 3 and 4.

Joints are defective in *Has2*-deficient limbs

In addition to skeletal defects, the *Has2*-deficient limbs possessed abnormal and defective joints. As shown in Fig. 3, the carpal, metacarpophalangeal and interphalangeal joints separating the skeletal elements of wild-type E16.5 autopods consist of thin well-demarcated bands or spaces representing the early synovial joint cavities. By contrast, the joint regions in the autopods of *Has2*-deficient mutant limbs were larger than normal and lacked distinct joint cavities (Fig. 3).

Histological sections through the carpal and phalangeal joints of E16.5 wild-type and *Has2* mutant autopods are shown in Fig. 4. The joints of the normal autopod consist of narrow well-defined spaces representing early joint cavities that contain only a few scattered cells (Fig. 4). By contrast, the joint regions in the autopods of the *Has2* mutant were filled with closely packed cells and distinct joint cavities were not evident (Fig. 4).

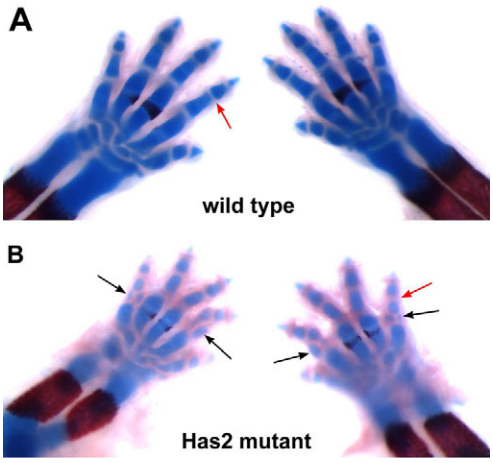

Fig. 3. Skeletal patterning and joint defects in the autopods of *Has2*-deficient limbs. Alcian Blue/Alizarin Red-stained E16.5 forelimb autopods of wild-type (**A**) and *Has2*-deficient (**B**) mouse limbs. The proximal phalanges of digits 2 and 5 are duplicated and misshapen in *Has2*-deficient autopods (black arrows in B). The *Has2*-deficient limbs also have abnormal joints. The joints separating the skeletal elements of wild-type E16.5 limbs consist of thin, well-demarcated, largely acellular bands representing the early synovial joint cavities (red arrow in A). The joint regions of the *Has2*-deficient mutant limbs are larger than normal and lack distinct joint cavities (red arrow in B).

The joints in the proximal regions of the *Has2* mutant limbs were also abnormal. As shown in Fig. 5, the shoulder and elbow joints of E16.5 wild-type embryos contain prominent and distinct acellular cavities. By contrast, the incipient joint cavities in the *Has2*-deficient shoulder and elbow joints were far smaller and less extensive and contained numerous cells (Fig. 5). Thus, in addition to the autopod defects, the formation of synovial joint cavities is defective in the proximal joints of *Has2* mutant limbs.

Growth plates are defective and disorganized in *Has2*-deficient skeletal elements

The growth plates of *Has2* mutant skeletal elements were severely disturbed and disorganized, and, in particular, normal cellular relationships were perturbed (Fig. 6). Firstly, as shown in Fig. 5, there was a considerable increase in cell density in *Has2*-deficient as compared with wild-type growth plates, reflecting a decrease in the amount of matrix separating the chondrocytes. This reduction in the amount of cartilage matrix in the mutant growth plates correlates with the striking decrease in the intensity of Alcian Blue staining of the cartilage matrix (see Figs 2 and 3), suggesting a decrease in the deposition of sulfated proteoglycans. Safranin O staining of glycosaminoglycans was also severely reduced in the *Has2* mutant growth plates and at P0 was limited to the central region of the growth plate, further indicating a decrease in the deposition of proteoglycans in the cartilage matrix (Fig. 7). Indeed, the deposition of aggrecan, the major sulfated proteoglycan of cartilage matrix, was severely reduced in the *Has2* mutant growth plates as assayed by immunostaining, and aggrecan deposition, like Safranin O staining, was limited to the center of the growth plate (Fig. 7). Although there was a decrease in cartilage matrix and in the deposition of aggrecan in the *Has2*-deficient growth plates, the expression of aggrecan transcripts, as detected by in situ hybridization, was comparable in wild-type and mutant growth

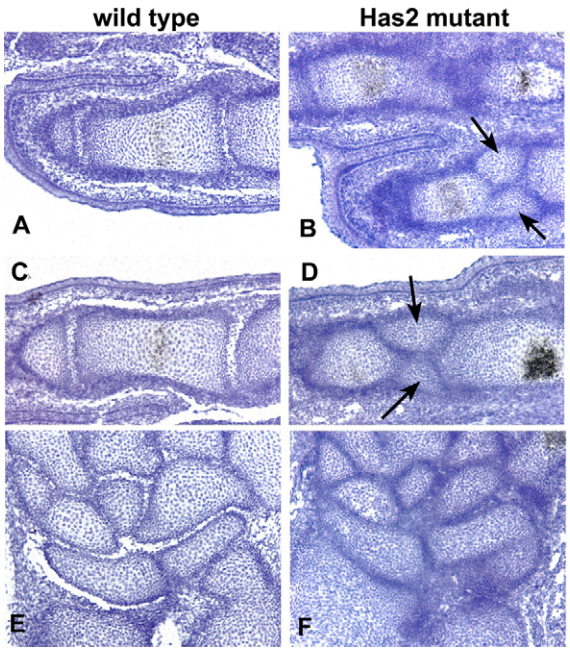

Fig. 4. Defective joint formation in the autopods of *Has2*-deficient limbs. Interphalangeal and metacarpophalangeal joints (**A-D**) and carpal and carpometacarpal joints (**E**,**F**) in E16.5 wild-type (A,C,E) and *Has2*-deficient (B,D,F) mouse autopods. The wild-type joints consist of narrow well-defined spaces representing early joint cavities that contain only a few scattered cells, whereas the joint regions in the *Has2* mutant are filled with closely packed cells and lack distinct joint cavities. Also note the duplicated proximal phalanges in the *Has2* mutant (arrows in B,D).

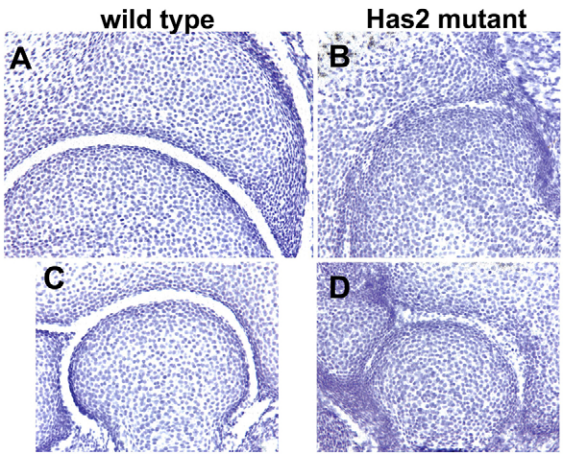

Fig. 5. Shoulder and elbow joints are defective in *Has2*-deficient limbs. Shoulder (**A**,**B**) and elbow (**C**,**D**) joints in E16.5 wild-type (A,C) and *Has2*-deficient (B,D) mouse limbs. Wild-type joints contain prominent and distinct acellular joint cavities, whereas the incipient joint cavities in the *Has2*-deficient joints are far smaller and less extensive than normal and contain numerous cells.

plates, as was the deposition of type II collagen as detected by immunostaining, although staining was somewhat reduced in the central region of the mutant growth plate (Fig. 7).

In addition to a decrease in proteoglycan deposition, normal cellular architecture and relationships were disrupted in the *Has2* mutant growth plates (Fig. 6). In wild-type growth plates, small, rounded resting and slowly proliferating chondrocytes at the epiphyseal end of the growth plate undergo a columnar differentiation process and form well-organized distinct longitudinal columns of flattened, highly proliferating chondrocytes (Koziel et al., 2005) (Fig. 6). In the *Has2*-deficient growth plates, this normal columnar organization was perturbed and distinct columns of chondrocytes were not evident (Fig. 6). The chondrocytes in the mutant growth plate were small, round and randomly distributed (Fig. 6).

Chondrocyte maturation is defective in *Has2*-deficient growth plates

In addition to the disruption of the normal columnar organization of the chondrocytes, there was a striking reduction in the number of hypertrophic chondrocytes detectable histologically in the *Has2*-deficient growth plates and in the proportion of chondrocytes that undergo hypertrophic maturation (Fig. 6). This indicates that the process of chondrocyte maturation, which plays a major role in the longitudinal growth of long bones, is perturbed in *Has2*-deficient growth plates. Consistent with this, in situ hybridization revealed that in E16.5 *Has2*-deficient growth plates there are striking reductions in the expression domains of type X collagen (*Col10a1*) (Fig. 8), a marker of definitive hypertrophic chondrocytes, and Indian hedgehog (*Ihh*), a marker of prehypertrophic chondrocytes (Fig. 9). The expression domains of *Ihh* and *Col10a1* were also severely reduced in P0 mutant growth plates (Fig. 10).

Although there was a striking reduction in the number of hypertrophic chondrocytes in the *Has2*-deficient growth plates, there was little or no difference in proliferation between the normal and *Has2* mutant growth plates as assayed by immunostaining for phosphorylated histone H3 (pHistoneH3) (Fig. 11). The proportion of pHistoneH3-stained nuclei in the metaphyseal regions of wild-type (3.5±0.7%; n=4) and *Has2* mutant (3.3±0.6%; n=4) growth plates was comparable.

Since hypertrophic chondrocyte maturation is perturbed in *Has2*-deficient growth plates, we aimed to determine whether there was a correlation between the expression of endogenous *Has2* in normal growth plates and the process of chondrocyte maturation. As shown in Fig. 12, in situ hybridization revealed that *Has2* expression is strongly upregulated at the onset of hypertrophic maturation in normal skeletal elements, concomitant with the conversion of immature proliferating chondrocytes into hypertrophying chondrocytes, a critical step in the maturation process. Thus, there is indeed a correlation between the temporal and spatial expression of *Has2* and the onset of hypertrophic maturation. Furthermore, biotinylated HABP staining revealed that in normal growth plates, hypertrophying chondrocytes are surrounded by prominent HA-rich pericellular coats (Fig. 13). By contrast, *Has2* expression, as assayed by in situ hybridization using an exon 2-specific probe, was not detectable in *Has2* mutant growth plates in which chondrocyte maturation was defective (Fig. 13), and little HABP staining was detectable in the *Has2*-deficient growth plates (Fig. 13).

The formation of the secondary ossification center is defective in *Has2*-deficient skeletal elements

The formation of a secondary ossification center is initiated at P9 in the growth plate of the normal humerus by the invasion of CD31 (Pcam1)-positive blood vessels into a zone of hypertrophic chondrocytes that differentiate in the central region of the growth

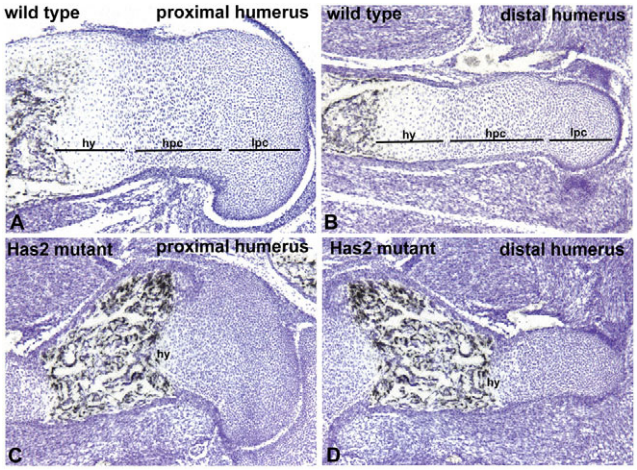

Fig. 6. Growth plates are defective and disorganized in *Has2*-deficient skeletal elements. Hematoxylin-stained sections through the growth plates of the proximal (**A**,**C**) and distal (**B**,**D**) humerus of E16.5 wild-type (A,B) and *Has2*-deficient (C,D) mouse limbs. The normal growth plates consist of zones of small, rounded, slowly proliferating chondrocytes (lpc), highly proliferating chondrocytes arranged in longitudinal columns (hpc), and hypertrophying chondrocytes (hy). The *Has2*-deficient growth plates are abnormal and disorganized: there is a decrease in the amount of matrix separating the cells, the normal columnar organization is perturbed and distinct columns of chondrocytes are not evident and, moreover, there is a striking reduction in the number of hypertrophic chondrocytes.

plate (Fig. 14). By contrast, in the P9 *Has2*-deficient humerus, a hypertrophic zone was not seen to differentiate in the central region of the growth plate, and vascular invasion into the growth plate was not detectable by CD31 immunostaining (Fig. 14). By P21, a large and prominent secondary ossification center was present in the normal humerus, but no secondary ossification center was observed in the *Has2*-deficient humerus (Fig. 14).

DISCUSSION

Has2-mediated production of HA is required for the longitudinal growth of limb skeletal elements and for the patterning of specific digital elements

In embryos and neonates in which the *Has2* gene has been conditionally inactivated in limb mesoderm, all of the skeletal elements in each of the segments of the forelimbs and hindlimbs are severely shortened, being about half the length of the normal skeletal elements. Thus, the Has2-mediated production of HA is necessary for the normal longitudinal growth of all of the skeletal elements of the limbs. The defect in the longitudinal growth of the *Has2*-deficient skeletal elements might result, at least in part, from the impaired progression of chondrocyte maturation, a process that plays a major role in the longitudinal growth of long bones (see below).

In addition to being severely shortened, *Has2*-deficient mutant limbs possess specific skeletal patterning defects. In particular, the proximal phalanges of digits 2 and 5 are duplicated and misshapen in the forelimbs and hindlimbs of all the *Has2* mutant E16.5 embryos and postnatal mice we have examined. In addition, the proximal phalanges of digits 3 and 4 are also partially duplicated in ~50% of the *Has2* mutant postnatal mice. Thus, Has2-mediated production of HA is involved in regulating the morphology and patterning of very specific portions of the digits. The fact that the duplications are limited to such specific digital elements is interesting, although the basis for this is not at all clear.

Has2-mediated production of HA is essential for the normal cellular organization of the growth plate

The growth plates of *Has2*-deficient skeletal elements are severely abnormal and disorganized. In particular, normal cellular architecture and relationships are perturbed. There is a decrease in the amount of matrix separating the chondrocytes in the *Has2* mutant growth plates, which is reflected in a considerable increase in cell density. The decrease in the amount of cartilage matrix results from a striking decrease in the deposition of sulfated proteoglycans, particularly aggrecan, as reflected in reduced Alcian Blue and Safranin O staining.

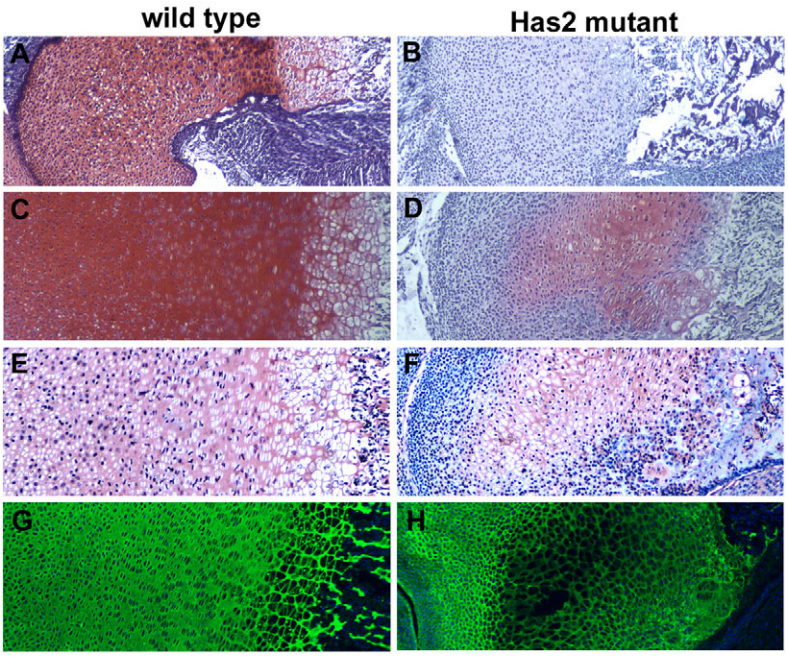

Fig. 7. Decreased deposition of proteoglycans particularly aggrecan in the matrix of *Has2*-deficient growth plates. Safranin O staining (**A-D**), aggrecan immunostaining (**E**,**F**) and type II collagen immunostaining (**G**,**H**) in the cartilage matrix of the growth plates of E16.5 (A,B) and P0 (C-H) wild-type (A,C,E,G) and *Has2*-deficient (B,D,F,H) mouse limbs. The deposition of glycosaminoglycans detectable by Safranin O staining (A-D) and aggrecan (E,F) is severely reduced in the *Has2* mutant growth plates. The deposition of type II collagen is comparable to that in the wild type (G) throughout most of the mutant growth plate (H), although staining is somewhat reduced in the center (H).

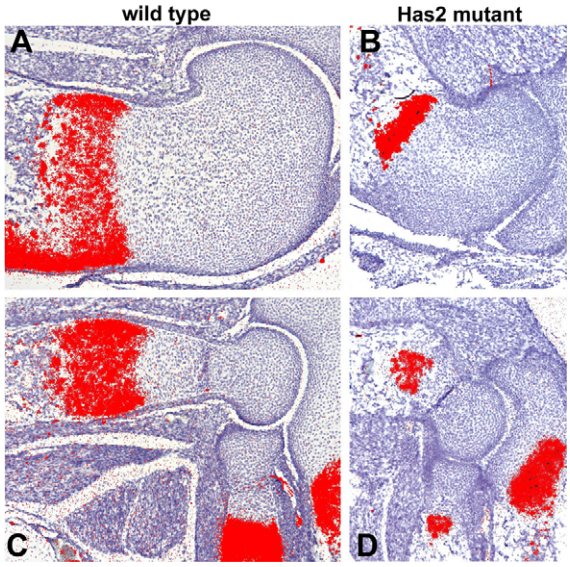

Fig. 8. The expression domain of the hypertrophic chondrocyte marker *Col10a1* is reduced in E16.5 *Has2*-deficient growth plates. *Col10a1* expression detected by in situ hybridization in the growth plates of the proximal (**A**,**B**) and distal (**C**,**D**) humerus of E16.5 wild-type (A,C) and *Has2* mutant (B,D) mouse limbs.

The decrease in cartilage matrix and in the deposition of sulfated proteoglycans, particularly aggrecan, in the *Has2*-deficient growth plates is very likely to be a consequence of the disruption of the large proteoglycan aggregates that are normally present in the matrix. In normal cartilage matrix, many aggrecan molecules bind to HA to form huge aggregates that give cartilage its tensile strength and elasticity. A reduction in the formation of proteoglycan aggregates due to defective HA production in the *Has2* mutant growth plates is very likely to result in the decreased deposition of aggrecan in the matrix.

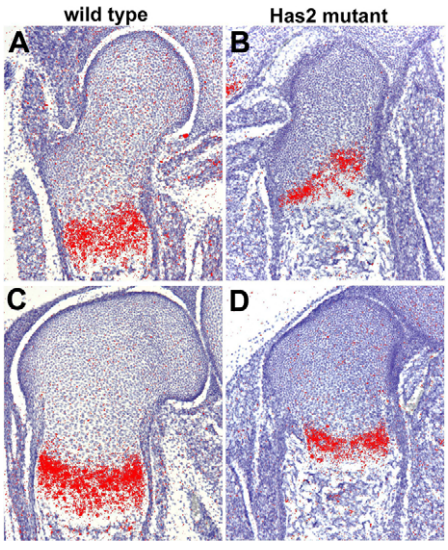

Fig. 9. The expression domain of the prehypertrophic chondrocyte marker *Ihh* is reduced in E16.5 *Has2*-deficient growth plates. *Ihh* expression detected by in situ hybridization in the growth plates of the proximal (**A**,**B**) and distal (**C**,**D**) femur of E16.5 wild-type (A,C) and *Has2* mutant (B,D) mouse limbs.

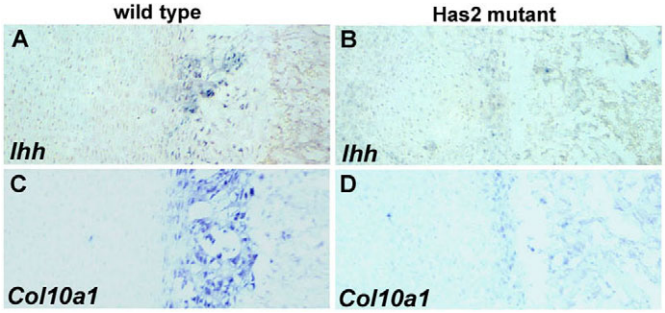

Fig. 10. Expression domains of *Ihh* and *Col10a1* are severely reduced in P0 *Has2*-deficient growth plates. *Ihh* (**A**,**B**) and *Col10a1* (**C**,**D**) expression detected by in situ hybridization in growth plates of P0 wild-type (A,C) and *Has2* mutant (B,D) mouse limbs.

Normal cellular organization and relationships are disrupted in the *Has2*-deficient growth plates. The epiphyseal ends of normal growth plates contain a zone of small, rounded, slowly proliferating chondrocytes that undergo a regulated columnar differentiation process to give rise to well-organized columns or stacks of flattened, highly proliferating chondrocytes (Koziel et al., 2005). However, in the *Has2* mutant growth plates, distinct columns of flattened chondrocytes are not present, and the mutant growth plate consists largely of small, rounded chondrocytes that are apparently randomly distributed. The organization of chondrocytes in columns or stacks along the longitudinal axis might be a factor in longitudinal growth (Karsenty and Wagner, 2002), so their altered orientation and disorganization in the *Has2*-deficient growth plates might contribute to the reduction in longitudinal growth.

The disorganization of normal columnar cellular relationships in the *Has2*-deficient growth plates might be a secondary consequence of the disruption of proteoglycan aggregates in the cartilage matrix. Similar growth plate disorganization occurs in mice deficient in link protein, which stabilizes aggregates of aggrecan and HA (Watanabe and Yamada, 1999), and in *cartilage matrix deficiency* (*cmd*) mice, which have a natural functional null mutation in the aggrecan gene (Schwartz and Domowicz, 2002; Watanabe and Yamada, 2003), as well as in *brachymorphic* (*bm*) mice, which possess undersulfated chondroitin sulfate proteoglycans (Cortes et al., 2009). Thus, the normal structural organization of the extracellular matrix might be necessary for maintaining normal cellular relationships and architecture. Another interesting possibility is that the perturbation of the normal columnar organization in the *Has2*-deficient growth plate might result from a perturbation in the signaling networks that regulate the columnar differentiation process (Koziel et al., 2005).

Has2-mediated production of HA is necessary for the normal progression of chondrocyte maturation

The longitudinal growth of the limb skeletal elements is dependent on a precisely regulated and coordinated program of chondrocyte maturation. During this process, immature proliferating chondrocytes are converted into postmitotic prehypertrophic chondrocytes, which undergo further maturation into hypertrophic chondrocytes that undergo apoptosis and are replaced by trabecular bone. Chondrocyte maturation is defective in *Has2*-deficient growth plates. In particular, there is a striking reduction in the number of hypertrophic chondrocytes and in the proportion of

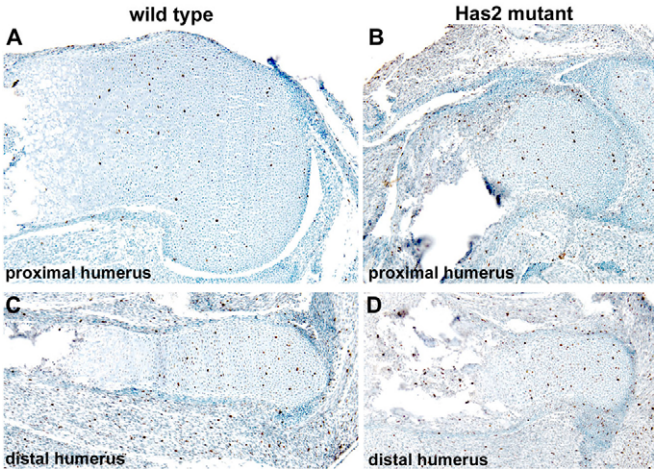

Fig. 11. Cell proliferation is comparable in wild-type and *Has2*-deficient growth plates. Cell proliferation assayed by phophorylated histone H3 (pHistoneH3) immunostaining in the growth plates of the proximal (**A**,**B**) and distal (**C**,**D**) humerus of E16.5 wild-type (A,C) and *Has2* mutant (B,D) mouse limbs. The proportion of pHistoneH3-stained nuclei is comparable in wild-type (A,C) (3.5±0.7%; *n*=4) and *Has2* mutant (B,D) (3.3±0.6%; *n*=4) growth plates.

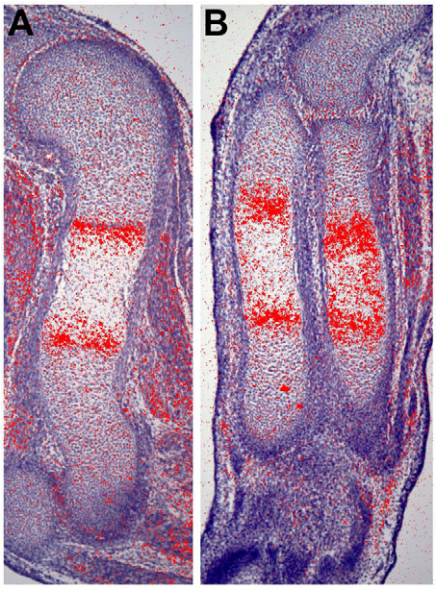

Fig. 12. *Has2* expression is upregulated at the onset of hypertrophic chondrocyte maturation. Expression of *Has2* detected by in situ hybridization in the humerus (**A**) and radius and ulna (**B**) of an E15 normal mouse limb. Expression of *Has2* is strongly upregulated at the onset of hypertrophic maturation, concomitant with the conversion of immature proliferating chondrocytes into hypertrophying chondrocytes.

chondrocytes that undergo hypertrophic maturation. The reduction in hypertrophic maturation is reflected in striking reductions in the expression domains of markers of hypertrophic differentiation, including *Ihh*, a marker of prehypertrophic chondrocytes, and *Col10a1*, a marker of definitive hypertrophic chondrocytes. These results indicate that defective hypertrophic chondrocyte maturation is a major factor in the impaired growth of skeletal elements in the *Has2*-deficient limbs. Moreover, the results indicate that Has2-mediated production of HA is necessary for the normal progression of chondrocyte maturation. Although there is a striking reduction in the number of hypertrophic chondrocytes in the *Has2*-deficient growth plates, there is little or no difference in cell proliferation between normal and *Has2* mutant growth plates, consistent with a severe impairment in the conversion of proliferating chondrocytes into hypertrophying chondrocytes. Taken together, these observations provide direct evidence of an important role for HA in chondrocyte maturation.

A crucial role for Has2-mediated production of HA in the regulation of chondrocyte maturation is supported by several other observations. In the present study, we have shown that *Has2* expression is strongly upregulated at the onset of hypertrophic maturation in normal skeletal elements during the conversion of immature proliferating chondrocytes into postmitotic prehypertrophic chondrocytes, a critical step in the maturation process. Others have also shown that *Has2* is the major HA synthase expressed in growth plate chondrocytes at the onset of hypertrophic maturation (Takeda et al., 1999; Suzuki et al., 2005; Schmidl et al., 2006). Moreover, we have confirmed the observations of others that hypertrophying chondrocytes are surrounded by HA-rich pericellular coats in which HA is bound to its receptor, CD44 (Knudson, 1993; Pavasant et al., 1996; Shibata et al., 2003; Knudson and Knudson, 2004; Suzuki et al., 2005). It has been suggested that the HA-rich pericellular coats may exert a swelling pressure that might aid in the expansion of the growth plate (Pavasant et al., 1996). Alternatively, we suggest that the interaction of pericellular HA with CD44 in hypertrophying chondrocytes might modulate or augment some of the signaling networks that regulate the progression of chondrocyte maturation. Significantly, in the chondrocytic cell line ATDC5, expression of *Has2* and *Runx2*, a crucial transcriptional regulator of chondrocyte maturation, is concomitantly upregulated at the onset of hypertrophic maturation (Tanne et al., 2008). Moreover, disruption of HA-CD44 interactions by addition of HA oligosaccharides or anti-CD44 antibodies inhibits *Runx2* expression, as well as the expression of hypertrophic markers including type X collagen (Tanne et al., 2008). These results further indicate that HA-CD44 interactions might indeed play an important role in regulating chondrocyte maturation.

HA is an important modulator or co-stimulator of signaling networks that have been implicated as positive regulators of chondrocyte maturation, including the BMP signal transduction pathway (Enomoto-Iwamoto et al., 1998; Volk et al., 1998; Grimsrud et al., 1999; Ito et al., 1999; Kameda et al., 2000; Volk et al., 2000; Bosky et al., 2002; Pogue and Lyons, 2006; Yoon et al., 2006). The upregulation of *Has2* expression at the onset of hypertrophic maturation correlates with the upregulation of *Bmp2* and *Bmp6* and with the activation of the transcriptional mediators of BMP signaling, Smad1, 5 and 8 (Yoon et al., 2006). Significantly, HA has been implicated as a modulator or co-activator of the BMP signaling network in articular chondrocytes, and may regulate cellular responsiveness to BMPs (Peterson et al., 2004). HA is also an important co-activator of the EGFR/ErbB signaling network, which has been implicated in the regulation of chondrocyte maturation (Fisher et al., 2007). Thus, it is possible that the interaction of pericellular HA with its receptors, including CD44, is involved in regulating hypertrophic maturation by co-activating or augmenting one or more of the signaling networks that regulate chondrocyte maturation.

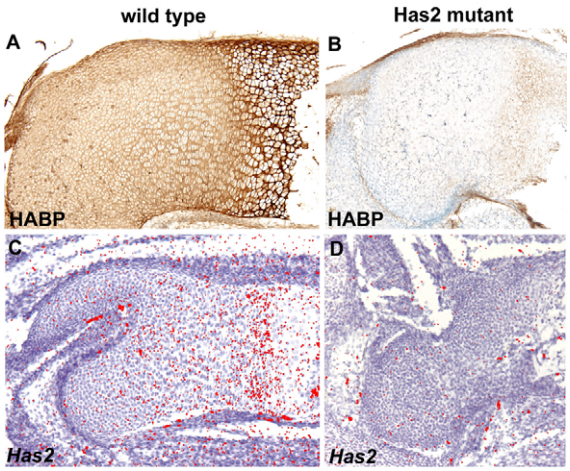

Fig. 13. Distribution of HA and *Has2* expression in wild-type and *Has2*-deficient growth plates. (**A**,**B**) HA detected by biotinylated HABP staining in the growth plates of the humerus of E16.5 wild-type (A) and *Has2*-deficient (B) mouse limbs. HA is distributed throughout the wild-type growth plate (A), but little HA is detectable in the *Has2* mutant growth plate (B). Note that the hypertrophying chondrocytes in the wild-type growth plate are surrounded by HA-rich pericellular coats (A). (**C**,**D**) *Has2* expression detected by in situ hybridization using an exon 2-specific probe in the growth plates of the femur of E16.5 wild-type (C) and *Has2*-deficient (D) limbs. Little or no *Has2* expression is detectable in the *Has2*-deficient growth plate. Note the upregulated expression of *Has2* at the onset of hypertrophic maturation in the wild-type growth plate (C) (see also Fig. 12).

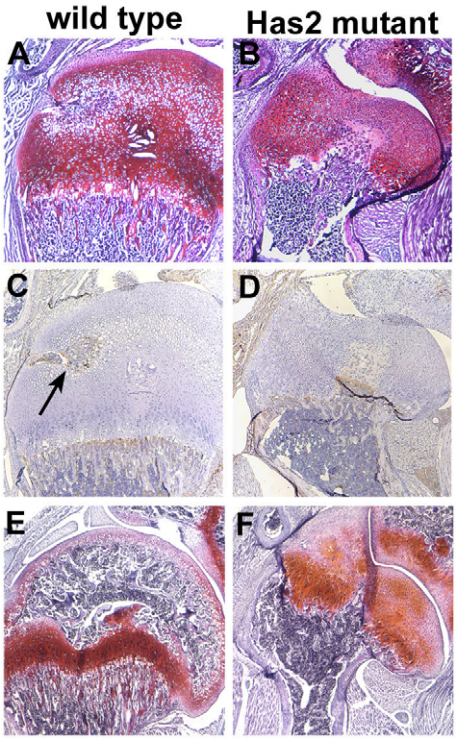

Fig. 14. Secondary ossification centers do not form in *Has2*-deficient growth plates. (**A**,**B**) Safranin O-stained P9 wild-type (A) and *Has2* mutant (B) mouse growth plates. A zone of hypertrophic chondrocytes is present in the central region of the wild-type growth plate (A), but not in the *Has2* mutant growth plate (B). (**C**,**D**) Vascular invasion detected by CD31 immunostaining in P9 wild-type (C) and *Has2* mutant (D) growth plates. CD31-positive blood vessels have invaded the central hypertrophic zone of wild-type growth plates (arrow in C), whereas vascular invasion has not occurred in the central region of the *Has2*-deficient growth plate (D). (**E**,**F**) P21 wild-type (E) and *Has2* mutant (F) growth plates. A prominent secondary ossification center is present in the wild-type growth plate (E), but not in the *Has2*-deficient growth plate (F).

Has2-mediated production of HA is necessary for the formation of secondary ossification centers

Our study has revealed an unexpected role for HA in the formation of the secondary ossification center. The secondary ossification center in the head of the normal humerus is formed by the invasion of blood vessels into a zone of hypertrophic chondrocytes that forms in the central regions of the growth plate. In the *Has2*-deficient humerus, a hypertrophic zone does not differentiate in the central region of the growth plate, vascular invasion does not occur, and a secondary ossification center does not form. It is likely that the lack of vascular invasion and inability to form the secondary ossification center are a direct consequence of the failure of hypertrophic differentiation in the *Has2*-deficient growth plate, as vascular invasion during endochondral ossification is dependent on Vegf and other factors produced by terminally differentiated hypertrophic chondrocytes (for a review, see Zelzer and Olsen, 2005). The lack of hypertrophic differentiation in the central region of the *Has2*-deficient growth plate further indicates that HA is an important regulator of hypertrophic chondrocyte maturation.

Has2-mediated production of HA plays a crucial role in joint formation

The onset of joint formation in the skeletal elements of the limb is characterized by the conversion of differentiated chondrocytes at sites of incipient joint formation into a narrow band of densely packed mesenchymal progenitor cells called the joint interzone (Archer et al., 2003; Pacifici et al., 2005). The interzone is the first morphological sign of overt joint formation, and the progenitor cells of the interzone ultimately give rise to articular cartilage and other components of synovial joints, including the synovial lining and joint ligaments (Rountree et al., 2004; Koyama et al., 2008). After formation of the interzone, the next critical step in joint formation is a cavitation process that results in the formation within the interzone of a cell-free fluid-filled space, which represents the future synovial cavity that leads to the separation of adjacent skeletal elements (Archer et al., 2003; Pacifici et al., 2005). In *Has2*-deficient limbs, the cavitation process that gives rise to the synovial cavities is defective. Distinct cavities are not present in the joint regions of the E16.5 autopods of *Has2* mutant limbs. Rather, the joint regions are wider than normal and filled with closely packed cells. The formation of synovial joint cavities is also defective in the proximal shoulder and elbow joints of the *Has2*-deficient limbs; the incipient joint cavities are considerably smaller and less extensive than normal and contain numerous cells. Thus, Has2-mediated production of HA is necessary for the cavitation process that results in the formation of the synovial joint cavities necessary for joint mobility.

Several other observations implicate HA in joint cavitation (for reviews, see Archer et al., 2003; Pacifici et al., 2005). We have found that *Has2* is expressed in developing joints, and relatively high amounts of HA are produced in the joint interzone prior to, and during, the cavitation process (Edwards et al., 1994; Archer et al., 2003). The HA receptor CD44 is also expressed in the joint

interzone, and perturbation of HA-CD44 interactions by exogenous small HA oligosaccharides impairs cavitation (Dowthwaite et al., 1998). It has been suggested that the localized synthesis and accumulation of high concentrations of HA, perhaps regulated by mechanical stimulation from muscle-driven movement, might facilitate the separation of interzone layers, thus promoting the formation of fluid-filled synovial cavities (Edwards et al., 1994; Archer et al., 2003). In any case, the defective cavitation evident in the *Has2*-deficient limbs provides direct evidence of a crucial role for Has2-mediated production of HA in joint formation and cavitation.

Acknowledgements
This work was supported by NIH grant HD022610 to R.A.K. and NS41332 and AR055670 to Y.Y. Deposited in PMC for release after 12 months.

References

Archer, C. W., Dowthwaite, G. P. and Francis-West, P. (2003). Development of synovial joints. *Birth Defects Res. C Embryo Today* **69**, 144-155.
Bosky, A. L., Paschalis, E. P., Binderman, I. and Doty, S. B. (2002). BMP-6 accelerates both chondrogenesis and mineral maturation in differentiating chick limb bud mesenchymal cell cultures. *J. Cell Biochem.* **84**, 509-519.
Bourguignon, L. Y. W., Zhu, H., Chu, A., Iida, N., Zhang, L. and Hung, M. C. (1997). Interaction between the adhesion receptor, CD44, and the oncogene product $p185^{HER2}$, promotes human ovarian tumor cell activation. *J. Biol. Chem.* **272**, 27913-27918.
Bourguignon, L. Y. W., Singleton, P. A., Zhu, H. and Zhou, B. (2002). Hyaluronan promotes signaling interactions between CD44 and the transforming growth factor β receptor I in metastatic breast tumor cells. *J. Biol. Chem.* **277**, 39703-39712.
Camenisch, T. D., Spicer, A. P., Brehm-Gibson, T., Biesterfeldt, J., Augustine, M. L., Calabro, A., Jr, Kubalak, S., Kelwer, S. E. and McDonald, J. A. (2000). Disruption of hyaluronan synthase-2 abrogates normal cardiac morphogenesis and hyaluronan-mediated transformation of epithelium to mesenchyme. *J. Clin. Invest.* **106**, 349-360.
Camenisch, T. D., Schroeder, J. A., Bradley, J., Klewer, S. E. and McDonald, J. A. (2002). Heart-valve mesenchyme formation is dependent on hyaluronan-augmented activation of ErbB2-ErbB3 receptors. *Nat. Med.* **8**, 850-855.
Coelho, C. N. D., Sumoy, L., Rodgers, B. J., Davidson, D. R., Hill, R. E., Upholt, W. B. and Kosher, R. A. (1991). Expression of the chicken homeobox-containing gene GHox-8 during embryonic chick limb development. *Mech. Dev.* **34**, 143-154.
Cortes, M., Baria, A. T. and Schwartz, N. B. (2009). Sulfation of chondroitin sulfate proteoglycans is necessary for proper Indian Hedgehog signaling in the developing growth plate. *Development* **136**, 1697-1706.
Dowthwaite, G. P., Edwards, J. C. W. and Pitsillides, A. A. (1998). An essential role for the interaction between hyaluronan and hyaluronan binding proteins during joint development. *J. Histochem. Cytol.* **46**, 641-651.
Edwards, J. C. W., Wilkinson, L. S., Jones, H. M., Soothill, P., Henderson, K. J., Worrall, J. G. and Pitsillides, A. A. (1994). The formation of human synovial joint cavities: a possible role for hyaluronan and CD44 in altered interzone cohesion. *J. Anat.* **185**, 355-367.
Enomoto-Iwamoto, M., Iwamoto, M., Mukudai, Y., Kawakami, Y., Nohno, T., Higuchi, Y., Takemoto, S., Ohuchi, H., Noji, S. and Kurisu, K. (1998). Bone morphogenetic protein signaling is required for maintenance of differentiated phenotype, control of proliferation, and hypertrophy in chondrocytes. *J. Cell Biol.* **140**, 409-418.
Fisher, M. C., Clinton, G. M., Maihle, N. J. and Dealy, C. N. (2007). Requirement for ErbB2/ErbB signaling in developing cartilage and bone. *Dev. Growth Differ.* **49**, 503-513.
Gakunga, P., Frost, G., Shuster, S., Cunha, G., Formby, B. and Stern, R. (1997). Hyaluronan is a prerequisite for ductal branching morphogenesis. *Development* **124**, 3987-3997.
Ghatak, S., Misra, S. and Toole, B. P. (2005). Hyaluronan constitutively regulates ErbB2 phosphorylation and signaling complex formation in carcinoma cells. *J. Biol. Chem.* **280**, 8875-8883.
Grimsrud, C. D., Romano, P. R., D'Souza, M., Puzas, J. E., Reynolds, P. R., Rosier, R. N. and O'Keefe, R. (1999). BMP-6 is an autocrine stimulator of chondrocyte differentiation. *J. Bone Miner. Res.* **14**, 475-481.
Inatani, M., Irie, F., Plump, A. S., Tessier-Lavigne, M. and Yamaguchi, Y. (2003). Mammalian brain morphogenesis and midline axon guidance require heparan sulfate. *Science* **302**, 1044-1046.
Itano, N., Sawai, T., Yoshida, M., Lenas, P., Yamada, Y., Imagawa, M., Shinomura, T., Hamaguchi, M., Yoshida, Y., Ohnuki, Y. et al. (1999). Three isoforms of mammalian hyaluronan synthases have distinct enzymatic properties. *J. Biol. Chem.* **274**, 25085-25092.
Ito, H., Akiyama, H., Shigeno, C. and Nakamura, T. (1999). Bone morphogenetic protein-6 and parathyroid hormone-related protein coordinately regulate the hypertrophic conversion in mouse clonal chondrogenic EC cells, ATDC5. *Biochim. Biophys. Acta* **1451**, 263-270.
Kameda, T., Koike, C., Saitoh, K., Kuroiwa, A. and Iba, H. (2000). Analysis of cartilage maturation using micromass cultures of primary chondrocytes. *Dev. Growth Differ.* **42**, 229-236.
Karsenty, G. and Wagner, E. F. (2002). Reaching a genetic and molecular understanding of skeletal development. *Dev. Cell* **2**, 389-406.
Knudson, C. B. (1993). Hyaluronan-receptor-directed assembly of chondrocyte pericellular matrix. *J. Cell Biol.* **120**, 825-834.
Knudson, C. B. and Toole, B. P. (1985). Changes in the pericellular matrix during differentiation of limb bud mesoderm. *Dev. Biol.* **112**, 308-318.
Knudson, C. B. and Knudson, W. (2004). Hyaluronan and CD44: modulators of chondrocyte metabolism. *Clin. Orthop. Relat. Res.* **427 Suppl.**, S152-S162.
Kosher, R. A. and Savage, M. P. (1981). Glycosaminoglycan synthesis by the apical ectodermal ridge of the chick limb bud. *Nature* **291**, 231-232.
Kosher, R. A., Savage, M. P. and Walker, K. H. (1981). A gradation of hyaluronate accumulation along the proximodistal axis of the embryonic chick limb bud. *J. Embryol. Exp. Morphol.* **63**, 85-98.
Koyama, E., Shibukawa, Y., Nagayama, M., Sugito, H., Young, G., Yuasa, T., Okabe, T., Ochiai, T., Kamiya, N., Rountree, R. B. et al. (2008). A distinct cohort of progenitor cells participates in synovial joint and articular cartilage formation during mouse limb skeletogenous. *Dev. Biol.* **316**, 62-73.
Koziel, L., Wuelling, M., Schneider, S. and Vortkamp, A. (2005). Gli3 acts as a repressor downstream of Ihh in regulating two distinct steps of chondrocyte differentiation. *Development* **132**, 5249-5260.
Lasko, M., Pichel, J. G., Gorman, J. R., Sauer, B., Okamoto, Y., Lee, E., Alt, F. W. and Westphal, H. (1996). Efficient *in vivo* manipulation of mouse genomic sequences at the zygote stage. *Proc. Natl. Acad. Sci. USA* **93**, 5860-5865.
Li, Y., Toole, B. P., Dealy, C. N. and Kosher, R. A. (2007). Hyaluronan in limb morphogenesis. *Dev. Biol.* **305**, 411-420.
Logan, M., Martin, J. F., Nagy, A., Lobe, C., Olson, E. N. and Tabin, C. J. (2002). Expression of Cre Recombinase in the developing mouse limb bud driven by a Prxl enhancer. *Genesis* **33**, 77-80.
Matsumoto, Y., Irie, F., Inatani, M., Tessier-Lavigne, M. and Yamaguchi, Y. (2007). Netrin-1/DCC signaling in commissural axon guidance requires cell-autonomous expression of heparan sulfate. *J. Neurosci.* **27**, 4342-4350.
McLeod, M. J. (1980). Differential staining of cartilage and bone in whole mount fetuses by Alcian blue and alizarin red S. *Teratology* **22**, 299-301.
Misra, S., Ghatak, S. and Toole, B. P. (2005). Regulation of MDR1 expression and drug resistance by a positive feedback loop involving hyaluronan, phosphoinositide 3-kinase, and ErbB2. *J. Biol. Chem.* **280**, 20310-20315.
Misra, S., Toole, B. P. and Ghatak, S. (2006). Hyaluronan constitutively regulates activation of multiple receptor tyrosine kinases in epithelial and carcinoma cells. *J. Biol. Chem.* **281**, 34936-34941.
Pacifici, M., Koyama, E. and Iwamoto, M. (2005). Mechanisms of synovial joint and articular cartilage formation: recent advances, but many lingering mysteries. *Birth Defects Res. C Embryo Today* **75**, 237-248.
Pavasant, P., Shizari, T. and Underhill, C. B. (1996). Hyaluronan contributes to the enlargement of hypertrophic lacunae in the growth plate. *J. Cell Sci.* **109**, 327-334.
Peterson, R. S., Andhare, R. A., Rousche, K. T., Knudson, W., Wang, W., Grossfield, J. B., Thomas, R. O., Hollingsworth, R. E. and Knudson, C. B. (2004). CD44 modulates Smad1 activation in the BMP-7 signaling network. *J. Cell Biol.* **166**, 1081-1091.
Pogue, R. and Lyons, K. (2006). BMP signaling in the cartilage growth plate. *Curr. Top. Dev. Biol.* **76**, 1-48.
Rountree, R. B., Schoor, M., Chen, H., Marks, M. E., Harley, V., Mishina, Y. and Kingsley, D. M. (2004). BMP receptor signaling is required for postnatal maintenance of articular cartilage. *PLoS Biol.* **2**, 1815-1827.
Schmidl, M., Adam, N., Surmann-Schmitt, C., Hattori, T., Stock, M., Dietz, U., de Crombrugghe, B., Poschl, E. and von der Mark, K. (2006). Twisted gastrulation modulates BMP-induced collagen II and X expression in chondrocytes *in vitro* and *in vivo*. *J. Biol. Chem.* **281**, 31790-31800.
Schwartz, N. B. and Domowicz, M. (2002). Chondrodysplasias due to proteoglycan defects. *Glycobiology* **12**, 57R-68R.
Sherman, L. S., Rizvi, T. A., Karyala, S. and Ratner, N. (2000). CD44 enhances neuregulin signaling by Schwann cells. *J. Cell Biol.* **150**, 1071-1083.
Shibata, S., Fukafa, K., Imai, H., Abe, T. and Yamashita, Y. (2003). In situ hybridization and immunohistochemistry of versican, aggrecan and link protein, and histochemistry of hyaluronan in developing mouse limb bud cartilage. *J. Anat.* **203**, 425-432.
Singley, C. T. and Solursh, M. (1981). The spatial distribution of hyaluronic acid and mesenchymal cell condensation in the embryonic chick wing. *Dev. Biol.* **84**, 102-120.

Spicer, A. P. and McDonald, J. A. (1998). Characterization and molecular evolution of a vertebrate hyaluronan synthase gene family. *J. Biol. Chem.* **273**, 1923-1932.
Suzuki, A., Tanimoto, K., Ohno, S., Nakatani, Y., Honda, K., Tanaka, N., Doi, T., Ohno-Nakahara, M., Yoneno, K., Ueki, M. et al. (2005). The metabolism of hyaluronan in cultured rabbit growth plate chondrocytes during differentiation. *Biochim. Biophys. Acta* **1743**, 57-63.
Takada, Y., Sakiyama, H., Kuriiwa, K., Masuda, R., Inoue, N., Nakagawa, K., Itano, N., Saito, T., Yamada, T. and Kimata, K. (1999). Metabolic activities of partially degenerated hypertrophic chondrocytes: Gene expression of hyaluronan synthases. *Cell Tissue Res.* **298**, 317-325.
Tammi, M. I., Day, A. J. and Turley, E. A. (2002). Hyaluronan and homeostasis: a balancing act. *J. Biol. Chem.* **277**, 4581-4584.
Tanne, Y., Tanimoto, K., Tanaka, N., Ueki, M., Lin, Y. Y., Ohkuma, S., Kamiya, T., Tanaka, E. and Tanne, K. (2008). Expression and activity of Runx2 mediated by hyaluronan during chondrocyte differentiation. *Arch. Oral Biol.* **53**, 478-487.
Toole, B. P. (1997). Hyaluronan in morphogenesis. *J. Intern. Med.* **242**, 35-40.
Toole, B. P. (2000a). Hyaluronan is not just a goo! *J. Clin. Invest.* **106**, 335-336.
Toole, B. P. (2000b). Hyaluronan in morphogenesis. *Semin. Cell Dev. Biol.* **12**, 79-87.
Toole, B. P., Wight, T. N. and Tammi, M. I. (2001). Hyaluronan-cell interactions in cancer and vascular disease. *J. Biol. Chem.* **277**, 4593-4596.
Tsatas, D., Kanagasundaram, V., Kaye, A. and Novak, U. (2002). EGF receptor modifies cellular responses to hyaluronan in glioblastoma cell lines. *J. Clin. Neurosci.* **9**, 282-288.
Turley, R. A., Nobel, P. W. and Bourguignon, L. Y. W. (2002). Signaling properties of hyaluronan receptors. *J. Biol. Chem.* **277**, 4589-4592.
Volk, S. W., Luvalle, P., Leask, T. and Leboy, P. S. (1998). A BMP responsive transcriptional region in the chicken type X collagen gene. *J. Bone Miner. Res.* **13**, 1521-1529.
Volk, S. W., D'Angelo, M., Diefenderfer, D. and Leboy, P. S. (2000). Utilization of bone morphogenetic protein receptors during chondrocyte maturation. *J. Bone Miner. Res.* **15**, 1630-1639.
Watanabe, H. and Yamada, Y. (1999). Mice lacking link protein develop dwarfism and craniofacial abnormalities. *Nature* **21**, 225-229.
Watanabe, H. and Yamada, Y. (2003). Chondrodysplasia of gene knockout mice for aggrecan and link protein. *Glycoconj. J.* **19**, 269-273.
Weigel, P. H., Hascall, V. C. and Tammi, M. (1997). Hyaluronan synthases. *J. Biol. Chem.* **272**, 13997-14000.
Wood, S. A., Allen, N. D., Rossant, J., Auerbach, A. and Nagy, A. (1993). Non-injection methods for the production of embryonic stem cell-embryo chimaeras. *Nature* **365**, 87-89.
Yoon, B. S., Pogue, R., Ovchinnikov, D. A., Yoshii, I., Mishina, Y., Behringer, R. R. and Lyons, K. M. (2006). BMPs regulate multiple aspects of growth-plate chondrogenesis through opposing actions on FGF pathways. *Development* **133**, 4667-4678.
Zelzer, E. and Olsen, B. R. (2005). Multiple roles of vascular endothelial growth factor (VEGF) in skeletal development, growth, and repair. *Curr. Top. Dev. Biol.* **65**, 169-187.